

A direct numerical simulation study of turbulence intensity effects on NO_x formation in freely propagating premixed flames

Shervin Karimkashi¹, Michele Bolla¹, Haiou Wang¹, Evatt R. Hawkes^{1,2}

¹School of Mechanical and Manufacturing Engineering,
University of New South Wales, NSW 2052 Australia

²School of Photovoltaic and Renewable Energy Engineering,
University of New South Wales, NSW 2052 Australia

Abstract

Direct numerical simulation (DNS) is utilized to study the effect of turbulence intensity on NO formation in two-dimensional (2D) freely propagating CH₄/air turbulent premixed flames in decaying isotropic turbulence. Chemical reactions are described by a reduced chemical kinetics mechanism for methane combustion based on GRI-Mech3.0, involving 28 species and 268 elementary reactions. Six DNS cases of different turbulent velocities were performed, with a constant turbulent length scale.

NO formation pathways for the low and high turbulence intensity cases are compared. In the low intensity case, all the pathways follow the trends of freely propagating laminar flame results. In the high intensity case, however, the pathway distributions are wider. Moreover, in highly turbulent flames, the net contribution of the prompt pathway, the main contributor for NO production in laminar flames and low turbulence intensity case, becomes negative, consuming NO. The reactions involved in the prompt pathway are analysed and compared with their laminar counterparts. It is concluded that in the high intensity case small turbulent eddies are able to transport some radicals to the higher temperature regions. Specifically, hydrocarbon radicals such as CH, CH₂ and CH₃, are transported to these regions where NO reacts with them.

Introduction

Turbulent premixed flames have been the focus of many studies for several decades due to their wide applications in transport and industry sectors, e.g. in internal combustion engines and gas turbines. NO_x emissions from the turbulent premixed flames combustion have been scrutinised for many years as one of the main concerns of fundamental and industrial communities [1-5]. These efforts have suggested using leaner operating conditions, to reduce NO_x formation, in practice. These lean (or ultra-lean) flames, however, are thicker and have lower laminar flame speeds that compel the engineers to use high turbulence intensity. In high turbulence intensities, the interactions between the small turbulent eddies and premixed flames becomes more significant because of a shorter Kolmogorov time scale compared with the chemical reactions timescales, which can be characterised by a high Karlovitz number, Ka [6]. Consequently, the inner thin reaction layer can be disrupted leading to a distributed combustion region of broken reaction zones; hence different NO formation pathways compared to the usual low turbulence intensities.

The recent studies by Carlsson et al. [7, 8] using 3D DNS approach for H₂/air and CH₄/air showed that for high Ka (high turbulence intensity) flames, the differential diffusion is decreased and that the chemical reaction pathways may be modified through activation of certain elementary reactions that

are less prominent at low Ka (e.g., $\text{H} + \text{CH}_2\text{O} \rightarrow \text{HCO}_2 + \text{H}_2$ for CH₄/air) by the intense turbulence redistributing heat and radicals. This effect resulted in a counter-intuitive observation of large heat release rate at low temperatures. They also showed that the reaction zones of the flames are thickened by turbulence but remains connected and not distributed. Also, recent studies of highly turbulent premixed flames by [9, 10], using 3D DNS for n-heptane/air flames have assessed the turbulence effects on differential diffusion and the effect of the nonlinear correlation between fuel consumption rate and curvature on the turbulent flame speed by performing simulations with both non-unity and unity Lewis numbers. Specifically, they are concluding that turbulence drives the effective species Lewis numbers towards unity through an increase in effective species and thermal diffusivities. Their work was continued later by using a detailed chemistry and also applying different unburnt temperatures and turbulence intensities to the same problem [11]. More recently, Wang et al. [12-14] reported the first DNS of an experimental high Ka premixed jet flame. The DNS results were compared to those from laser-based diagnostics with good agreement [12]. Physical insights were provided into the flame structure to understand the substantial flame broadening that is observed in both the experiment and DNS [13]. In Wang et al. [14], the roles of unsteady flame curvature and straining on flame propagating and the flame stabilisation were discussed and the sensitivity of the results on different species were also investigated.

Despite the available experimental and numerical studies of highly turbulent premixed combustion, there is a gap to analyse the interactions between the strong turbulence and chemical reactions in the context of the NO formation pathways. As chemical reactions can be modified by the small turbulent eddies, it is essential to investigate the mechanism how they can affect the NO formation. With no experimental and modelling studies available for exploring the NO formation pathways in high turbulence intensity cases, the technique of direct numerical simulation (DNS) has a role to play to help fill this knowledge gap.

This paper presents the effects of high turbulence intensity on the NO formation and the NO reaction pathways through a 2D DNS approach for lean methane/air combustion. The DNS solver and the governing equations are introduced in section 2. A laminar premixed flame and several turbulent premixed flames with different turbulence intensities are chosen to perform this study and they are introduced in section 3. In Section 4, results and discussion are presented. In particular, the influence of high turbulence intensity on NO pathways is evaluated and the modified reactions are identified. Finally, some conclusions are made in Section 5.

Governing Equations

The code for turbulent premixed flame calculations used here is a DNS code called S3D, which has been used for numerous studies, e.g. [15-18]. It solves the transport equations for continuity, momenta, species mass fractions and total energy. S3D uses 8th order explicit finite differencing spatial scheme [19], and 4th order explicit Runge-Kutta time integration method [20]. The Navier-Stokes characteristic boundary condition (NSCBC) was employed for all the boundaries [21]. Chemical reactions are described by a reduced chemical kinetics mechanism for methane combustion based on GRI-Mech3.0, involving 28 species and 268 elementary reaction steps [22].

Numerical tests

The appropriate operating conditions with CO₂-diluted and oxygen-enriched premixed methane-air in the gas turbine have been proposed by previous researches [23, 24] based on the performance efficiency and the gas turbine design limitations. The content of CO₂ dilution and O₂ enrichment as well as the inlet temperature and equivalence ratio in this study are chosen from conditions suggested in Ref. [24]. The composition chosen in this study is methane-air diluted with 7.5% O₂ enrichment and 30% CO₂ dilution in volume fraction. The reactant temperature is 600 K and the reactant composition is homogenous with an equivalence ratio of 0.7. At the given conditions and atmospheric pressure, the adiabatic flame temperature is 1871 K.

The 2D simulations are initialised with the converged results of a freely propagating laminar premixed flame. Therefore, the initial NO (and other species) mass fraction for the 2D case is obtained from the converged solution in the 1D laminar simulation. A 1D freely propagating laminar flame with the same initial conditions and composition has been considered as the laminar case in this study.

In order to study the effects of turbulence intensity on NO formation, turbulence velocity ratio is gradually increased on the regime diagram from corrugated flamelet zone to the thin reaction zone and finally to the broken reaction zone with a constant length-scale ratio. These cases are summarised in table 1. The laminar flame speed and flame thickness are $S_L = 0.3595$ m/s and $\delta_f = 0.6$ mm, respectively. Up and Lt are turbulence velocity and turbulence length-scale, respectively.

Case	Up/S _L	Lt/δ _f	Up (m/s)	Lt (mm)	Eddy turn-over time
1	1.5	9	0.54	5.4	1.0e-2
2	5	9	1.8	5.4	3.0e-3
3	20	9	7.18	5.4	7.51e-4
4	40	9	14.4	5.4	3.76e-4
5	90	9	32.4	5.4	1.67e-4
6	200	9	71.9	5.4	7.51e-5

Table 1. The DNS cases and their characteristics

A low turbulence intensity case and a high turbulence intensity case are selected to be compared in this study, which are case 2 - on the border between the corrugated flamelet zone and thin reaction zone - and case 6 - in the broken reaction zone.

Results and discussion

Figure 1 shows the NO formation pathways for the corresponding freely propagating laminar case. It is observed that NO₂ pathway is consuming the NO diffused to the preheat zone from downstream but it produces NO in the fuel consumption zone. Prompt pathway has the main contribution for NO production with a peak in the reaction zone. Thermal pathway is also important with a peak in the fuel consumption zone and its contribution subsists in the oxidation zone. N₂O pathway has a smaller contribution for NO production. These results are consistent with the previous results of [25] for a lean premixed laminar methane flame.

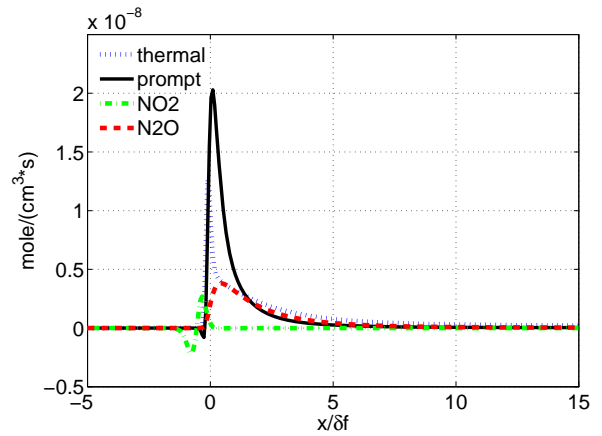


Figure 1. Different pathways of NO formation for the 1D laminar flame

The NO pathways for turbulent cases are analysed and compared with those of the freely propagating laminar case and displayed in figure 2 and figure 3 for case2 (low turbulence intensity) and case6 (highest turbulence intensity), respectively. In case2, although the prompt pathway demonstrates an increase in the peak value compared with the laminar case, all the pathways display a similar trend as in the laminar case. In case6, however, the pathways are more scattered, as expected, due to the higher turbulence intensity leading to a higher level of mixing. More interestingly, it is observed that as the turbulence intensity is increased, the prompt pathway, which is the main contributor for NO formation, approaches to negative values, in contrast to its NO production in laminar and weakly turbulent premixed flames.

As the prompt pathway is the dominant pathway and its modification with the high turbulence intensity is more considerable than the other pathways, it will be the focus of this study to clarify the reason for this major modification.

The potential reason of the observed negative values for the prompt pathway in case6 can be the modification of some local chemical reactions involved in the prompt pathway, due to the fast transport of the small structures of the intermediate radicals to the high temperature regions, in such a high turbulence intensity. In order to examine the potential modifications of the local chemical reactions involved in the prompt pathway, caused by the high turbulence intensity, some key elementary reactions of the DNS are compared with their laminar counterparts.

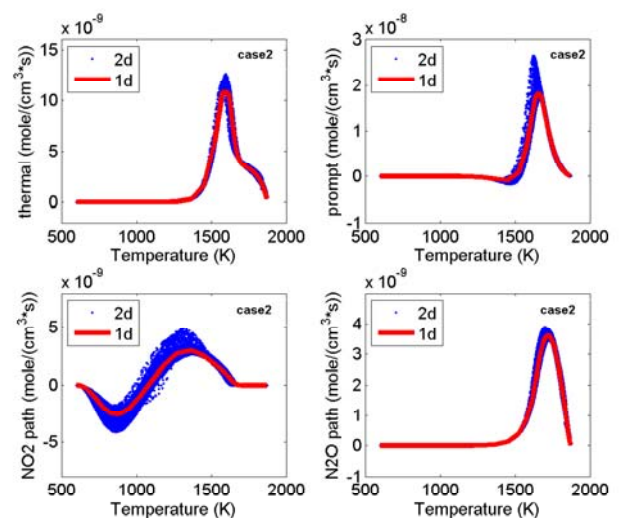


Figure 2. NO pathways for the low turbulence intensity case (case2)

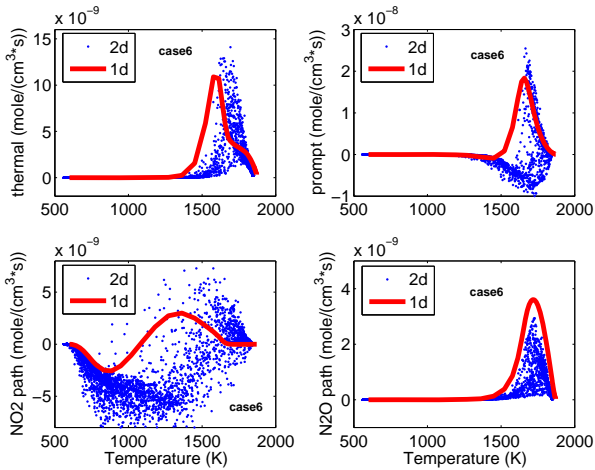


Figure 3. NO pathways for the high turbulence intensity case (case6)

Table 2 displays all the prompt pathway chemical reactions with their corresponding reaction numbers as they appear in the chemical mechanism used in this study. By considering these local intermediate reactions for the laminar or turbulent cases, it was observed that some of them have negative reaction rates while some others have positive reaction rates (not shown here). These negative and positive reaction rates compete and lead to a positive or negative net value for the prompt pathway. For the laminar case or the low turbulent intensity case, the reaction rates with negative values are an order of magnitude smaller than those with positive values, leading to a positive net value for the prompt pathway. However, in the high turbulence intensity case (case6), the reactions with negative reaction rates become more than an order of magnitude bigger (compared to their values in the laminar case) while the reactions with positive values do not modify significantly. Consequently, the prompt pathway in case6 becomes negative in some regions. Here, we only show one example of the several reactions with negative reaction rates. Figure 4 compares the reaction rate for the local reaction No. 231 in case6 with its counterpart in the laminar case. In the high turbulence intensity case (case6), the negative rate of this reaction has become an order of magnitude higher (more negative) which makes it stronger in competition with the positive reaction rates.

178. $\text{NH}+\text{O} \rightleftharpoons \text{NO}+\text{H}$	212. $\text{NCO}+\text{NO} \rightleftharpoons \text{N}_2+\text{CO}_2$
183. $\text{NH}+\text{O}_2 \rightleftharpoons \text{NO}+\text{OH}$	223. $\text{C}+\text{NO} \rightleftharpoons \text{CO}+\text{N}$
186. $\text{NH}+\text{NO} \rightleftharpoons \text{N}_2+\text{OH}$	224. $\text{CH}+\text{NO} \rightleftharpoons \text{HCN}+\text{O}$
196. $\text{NNH}+\text{O} \rightleftharpoons \text{NH}+\text{NO}$	225. $\text{CH}+\text{NO} \rightleftharpoons \text{H}+\text{NCO}$
200. $\text{H}+\text{NO}+\text{M} \rightleftharpoons \text{HNO}+\text{M}$	226. $\text{CH}+\text{NO} \rightleftharpoons \text{N}+\text{HCO}$
201. $\text{HNO}+\text{O} \rightleftharpoons \text{NO}+\text{OH}$	227. $\text{CH}_2+\text{NO} \rightleftharpoons \text{H}+\text{HNCO}$
202. $\text{HNO}+\text{H} \rightleftharpoons \text{H}_2+\text{NO}$	228. $\text{CH}_2+\text{NO} \rightleftharpoons \text{OH}+\text{HCN}$
203. $\text{HNO}+\text{OH} \rightleftharpoons \text{NO}+\text{H}_2\text{O}$	229. $\text{CH}_2(\text{S})+\text{NO} \rightleftharpoons \text{H}+\text{HNCO}$
204. $\text{HNO}+\text{O}_2 \rightleftharpoons \text{HO}_2+\text{NO}$	230. $\text{CH}_2(\text{S})+\text{NO} \rightleftharpoons \text{OH}+\text{HCN}$
205. $\text{NCO}+\text{O} \rightleftharpoons \text{NO}+\text{CO}$	231. $\text{CH}_3+\text{NO} \rightleftharpoons \text{HCN}+\text{H}_2\text{O}$
207. $\text{NCO}+\text{OH} \rightleftharpoons \text{NO}+\text{H}+\text{CO}$	232. $\text{CH}_3+\text{NO} \rightleftharpoons \text{H}_2\text{CN}+\text{OH}$
209. $\text{NCO}+\text{O}_2 \rightleftharpoons \text{NO}+\text{CO}_2$	249. $\text{N}+\text{CO}_2 \rightleftharpoons \text{NO}+\text{CO}$

Table 2. List of the reactions involved in the prompt pathway

By considering all the local reactions with negative reaction rate values, those reactions that their negative reaction rate values are considerably increased in the high turbulence intensity case (case6) have either of three unburned intermediate radicals of fuel, CH, CH₂ and CH₃ in common. This implies that the transport of these unburned intermediate fuel radicals to the high temperature regions is the main cause for the negative reaction rates enhancement. For example, in the reaction No. 231, CH₃ is consuming NO. In the highly turbulent case, CH₃ is transported to the high temperature region (where more NO exists); hence more NO is consumed (i.e. more negative reaction rate).

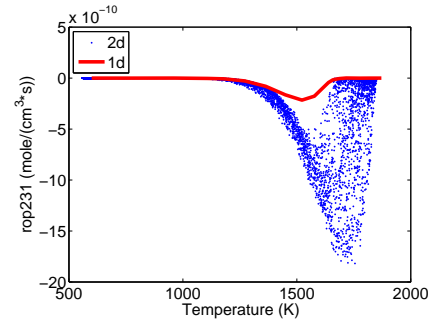


Figure 4. Reaction rate for the laminar case and the high turbulence intensity case (case6)

To clarify this effect more rigorously, we study the mass fractions of these intermediate radicals in the low and high turbulence intensity cases.

The contours of CH₃ mass fractions are displayed in figure 5 for case2 and also in figure 6 for case6. These two figures demonstrate that in case2, where the turbulence intensity is lower, the concentration of CH₃ (also CH₂ and CH, not shown here) follows the iso-line of T=1400 K, specified by the black line in the figure.

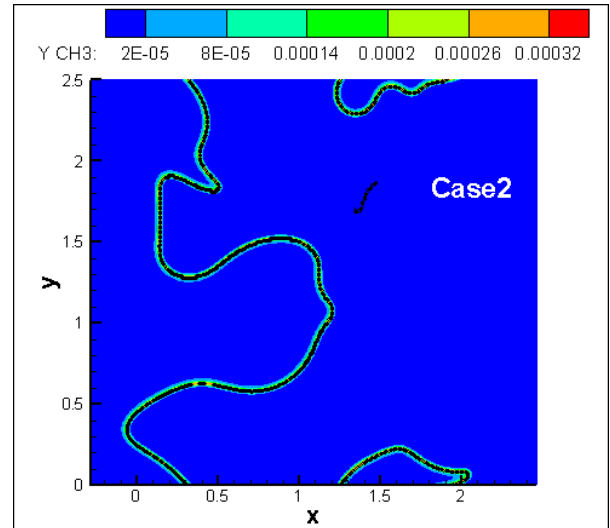


Figure 5. Contours of CH₃ mass fraction in the low turbulence intensity case (case2) – the black line is representing the iso-line for T = 1400 K

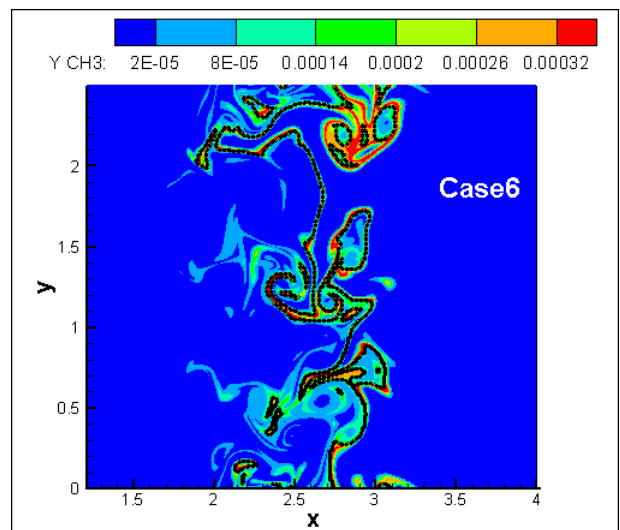


Figure 6. Contours of CH₃ mass fraction in the high turbulence intensity case (case6) – the black line is representing the iso-line for T = 1400 K

In case6 (figure 6), however, the small eddies of turbulence are able to transport CH₃ (also CH₂ and CH, not shown here) radicals to the regions with higher temperature (higher than 1400 K) where more NO is present. Therefore, in the highly turbulent case (compared to the low turbulence intensity case or the laminar case), the concentrations of CH₃, CH₂ and CH are higher in the high temperature regions. As NO is mainly found in those high temperature regions, reactions like reaction No. 231 will be reactivated and this leads to the higher consumption of NO (more negative reaction rate in figure 4) compared to the low turbulence intensity case or the laminar case.

Conclusions

DNS was utilised to study the NO formation pathways in two-dimensional (2D) freely propagating CH₄/air turbulent premixed flames with decaying isotropic turbulence. It was shown that in the highly turbulent flames, the NO formation pathways are different than in the low turbulence intensity or freely propagating laminar flames; especially for the prompt pathway. With the increase of the turbulence intensity, the prompt pathway which is the main contributor for NO production for the laminar and low turbulence intensity cases, approaches to negative values, in contrast to what was observed for laminar and low turbulence intensity cases. The negative prompt pathway observed in the highly turbulent case, is originated from the modifications of some local intermediate reactions, with negative reaction rates, involved in the prompt pathway. In the high turbulence intensity case, these reactions (with negative reaction rates) are able to compete with the other reactions (with positive reaction rates) and to consume more NO compared to the low turbulence intensity case or the freely propagating laminar case. This modification of the local intermediate reactions is the result of stronger convection and diffusion terms (the shorter scalar transport timescale) in the highly turbulent case, compared with the low intensity turbulence case or the freely propagating laminar case. These strong scalar transport terms can transport the unburned local intermediate radicals of fuel, namely CH, CH₂ and CH₃, to the high temperature regions where they can react with the NO species (having high concentrations in those high temperature regions) and consume more NO; which leads to the negative NO prompt pathway in the highly turbulent case.

Acknowledgments

This research was sponsored by funding from the Australian Renewable Energy Agency (ARENA). Computational resources were provided under the National Computational Merit Allocation Scheme at the Australian National Computational Infrastructure Facility and at the Pawsey Supercomputing Centre, and also provided by Intersect Australia Pty Ltd and the UNSW Faculty of Engineering.

References

[1] S. M. Cannon, B. S. Brewster and L. D. Smoot, Stochastic Modeling of CO and NO in Premixed Methane Combustion, *Combust. Flame* **113** (1–2) 1998, 135-146.
 [2] H. P. Mallampalli, T. H. Fletcher and J. Y. Chen, Evaluation of CH₄/NO_x Reduced Mechanisms Used for Modeling Lean Premixed Turbulent Combustion of Natural Gas, *J. Eng. Gas Turbines Power* **120** (4) 1998, 703-712.
 [4] M. S. Day, J. B. Bell, X. Gao and P. Glarborg, Numerical simulation of nitrogen oxide formation in lean premixed turbulent H₂/O₂/N₂ flames, *Proc. Combust. Inst.* **33** (1) 2011, 1591-1599.

[5] J. B. Bell, M. S. Day and M. J. Lijewski, Simulation of nitrogen emissions in a premixed hydrogen flame stabilized on a low swirl burner, *Proc. Combust. Inst.* **34** (1) 2013, 1173-1182.
 [6] N. Peters, The turbulent burning velocity for large-scale and small-scale turbulence, *J. Fluid Mech.* **384** 1999, 107-132.
 [7] H. Carlsson, R. Yu and X.-S. Bai, Direct numerical simulation of lean premixed CH₄/air and H₂/air flames at high Karlovitz numbers, *Int. J. Hydrogen Energy* **39** (35) 2014, 20216-20232.
 [8] H. Carlsson, R. Yu and X.-S. Bai, Flame structure analysis for categorization of lean premixed CH₄/air and H₂/air flames at high Karlovitz numbers: Direct numerical simulation studies, *Proc. Combust. Inst.* **35** (2) 2015, 1425-1432.
 [9] B. Savard, B. Bobbitt and G. Blanquart, Structure of a high Karlovitz n-C₇H₁₆ premixed turbulent flame, *Proc. Combust. Inst.* **35** (2) 2015, 1377-1384.
 [10] B. Savard and G. Blanquart, Broken reaction zone and differential diffusion effects in high Karlovitz n-C₇H₁₆ premixed turbulent flames, *Combust. Flame* **162** (5) 2015, 2020-2033.
 [11] S. Lapointe, B. Savard and G. Blanquart, Differential diffusion effects, distributed burning, and local extinctions in high Karlovitz premixed flames, *Combust. Flame* **162** (9) 2015, 3341-3355.
 [12] H. Wang, E. R. Hawkes, B. Zhou, J. H. Chen, Z. Li and M. Aldén, A comparison between direct numerical simulation and experiment of the turbulent burning velocity-related statistics in a turbulent methane-air premixed jet flame at high Karlovitz number, *Proc. Combust. Inst.* doi: **10.1016/j.proci.2016.07.104** 2016,
 [13] H. Wang, E. R. Hawkes, J. H. Chen, B. Zhou, Z. Li and M. Aldén, Petascale direct numerical simulations of a high Ka laboratory premixed jet flame – an analysis of flame stretch and flame thickening, *J. Fluid Mech.* **under review** 2016,
 [14] H. Wang, E. R. Hawkes and J. H. Chen, A direct numerical simulation study of flame structure and stabilisation of an experimental high Ka CH₄/air premixed jet flame, *Combust. Flame* **under review** 2016,
 [15] E. R. Hawkes and J. H. Chen, Direct numerical simulation of hydrogen-enriched lean premixed methane-air flames, *Combust. Flame* **138** (3) 2004, 242-258.
 [16] A. Krisman, E. R. Hawkes, M. Talei, A. Bhagatwala and J. H. Chen, Polybrachial structures in dimethyl ether edge-flames at negative temperature coefficient conditions, *Proc. Combust. Inst.* **35** (1) 2015, 999-1006.
 [17] S. Karami, E. R. Hawkes, M. Talei and J. H. Chen, Mechanisms of flame stabilisation at low lifted height in a turbulent lifted slot-jet flame, *J. Fluid Mech.* **777** 2015, 633-689.
 [18] A. Gruber, R. Sankaran, E. R. Hawkes and J. H. Chen, Turbulent flame-wall interaction: a direct numerical simulation study, *J. Fluid Mech.* **658** 2010, 5-32.
 [19] S. K. Lele, Compact finite difference schemes with spectral-like resolution, *J. Comput. Phys.* **103** (1) 1992, 16-42.
 [20] C. A. Kennedy, M. H. Carpenter and R. M. Lewis, Low-storage, explicit Runge-Kutta schemes for the compressible Navier-Stokes equations, *Appl. Numer. Math.* **35** (3) 2000, 177-219.
 [21] C. S. Yoo and H. G. Im, Characteristic boundary conditions for simulations of compressible reacting flows with multi-dimensional, viscous and reaction effects, *Combust. Theor. Model.* **11** (2) 2007, 259-286.
 [22] T. Lu and C. K. Law, A criterion based on computational singular perturbation for the identification of quasi steady state species: A reduced mechanism for methane oxidation with NO chemistry, *Combust. Flame* **154** (4) 2008, 761-774.
 [23] S. de Persis, G. Cabot, L. Pillier, I. Gökalp and A. M. Boukhalfa, Study of Lean Premixed Methane Combustion with CO₂ Dilution under Gas Turbine Conditions, *Energy & Fuels* **27** (2) 2013, 1093-1103.
 [24] S. de Persis, F. Foucher, L. Pillier, V. Osorio and I. Gökalp, Effects of O₂ enrichment and CO₂ dilution on laminar methane flames, *Energy* **55** 2013, 1055-1066.
 [25] M. Nishioka, S. Nakagawa, Y. Ishikawa and T. Takeno, NO emission characteristics of methane-air double flame, *Combust. Flame* **98** (1) 1994, 127-138.